Nanoscale

RSC Publishing

PAPER

View Article Online
View Journal | View Issue

Cite this: *Nanoscale*, 2013, **5**, 687

Targeted nanoparticles for enhanced X-ray radiation killing of multidrug-resistant bacteria†

Yang Luo,[ab] Mainul Hossain,[b] Chaoming Wang,[b] Yong Qiao,[b] Jincui An,[b] Liyuan Ma[b] and Ming Su*[b]

Received 12th October 2012
Accepted 20th November 2012

DOI: 10.1039/c2nr33154c

www.rsc.org/nanoscale

This paper describes a nanoparticle enhanced X-ray irradiation based strategy that can be used to kill multidrug resistant (MDR) bacteria. In the proof-of-concept experiment using MDR *Pseudomonas aeruginosa* (*P. aeruginosa*) as an example, polyclonal antibody modified bismuth nanoparticles are introduced into bacterial culture to specifically target *P. aeruginosa*. After washing off uncombined bismuth nanoparticles, the bacteria are irradiated with X-rays, using a setup that mimics a deeply buried wound in humans. Results show that up to 90% of MDR *P. aeruginosa* are killed in the presence of 200 μg ml^{-1} bismuth nanoparticles, whereas only ~6% are killed in the absence of bismuth nanoparticles when exposed to 40 kVp X-rays for 10 min. The 200 μg ml^{-1} bismuth nanoparticles enhance localized X-ray dose by 35 times higher than the control with no nanoparticles. In addition, no significant harmful effects on human cells (HeLa and MG-63 cells) have been observed with 200 μg ml^{-1} bismuth nanoparticles and 10 min 40 kVp X-ray irradiation exposures, rendering the potential for future clinical use. Since X-rays can easily penetrate human tissues, this bactericidal strategy has the potential to be used in effectively killing deeply buried MDR bacteria *in vivo*.

1 Introduction

Treating multidrug-resistant (MDR) bacterial infection is challenging in a deep wound situation. Due to the concern of increased drug resistance evolved from various antibiotics, physical antimicrobial agents with high efficiency are receiving more attention. Silver nanoparticles can be added into bandages to prevent infection and facilitate wound healing.[1] Gold nanoparticles have been used to enhance photo-thermal based bacterial killing.[2–4] Although these methods can kill bacteria from superficial wounds, they are less effective in eradicating bacteria that are deeply buried underneath the dermis. Recently, silver nanoparticle sandwich nanostructures have been developed as bacteriostatic implant coatings,[5] but the controlled release of silver ions is still challenging.

Ionizing radiation including X-rays and gamma rays can easily penetrate most tissues and kill bacteria by inducing irreparable DNA damage.[6] Many Gram-negative bacteria such as *Pseudomonas aeruginosa* (*P. aeruginosa*), *Escherichia coli* (*E. coli*) and *Salmonella* species can be effectively killed by X-rays *in vitro*. More recently, high energy X-ray radiation has also been developed to eliminate bacteria in living oysters without killing the oysters, revealing the possibility of X-ray based bacterial killing in living objects. However, no such X-ray radiation-induced bactericidal strategies have been carried out *in vivo* due to concerns of high dose irradiation exposure.

Nanoparticles of heavy elements (such as gold and bismuth), having a large cross-section for X-ray absorption and photoelectron generation, can be used as radiosensitizers to enhance the radiation dose for bacterial killing.[7–9] Free radicals and photoelectrons that are generated by X-ray irradiation of the nanoparticles contribute to significant DNA damage in the bacteria. If damaged DNAs are not repaired by enzymes in bacteria, damage can be accumulated, eventually causing bacterial death. The bacterial killing effect is significantly influenced by the distance between nanoparticles and bacteria due to a short diffusion length (~100 nm) of free radicals under physiological conditions. This is evident from previous studies using unconjugated gold nanoparticles which required a high dose (~100 Gy) to kill bacteria.[10] Meanwhile, targeted gold nanoparticles attached to the bacterial cell surface have shown higher antimicrobial activity than non-targeted nanoparticles using a photothermal effect.[11] However, this method is limited by low penetrating power of visible light and cannot be used for treating deeply buried bacteria.

This paper describes a novel bactericidal approach to kill MDR bacteria using low dose X-rays and antibody conjugated bismuth nanoparticles that can specifically be targeted on bacterial surfaces. Since X-rays are highly penetrating, this method has the potential to kill bacteria inside deep tissues.

[a]*Department of Laboratory Medicine, Southwest Hospital, Third Military Medical University, Chongqing 400038, China*

[b]*NanoScience Technology Center, University of Central Florida, Orlando, Florida 32826, USA. E-mail: ming.su@ucf.edu*

† Electronic supplementary information (ESI) available. See DOI: 10.1039/c2nr33154c

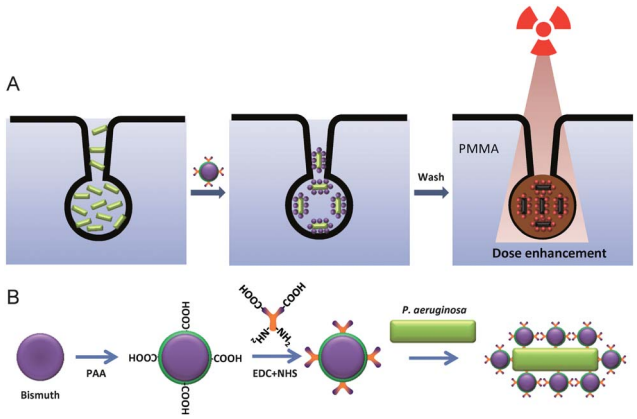

Fig. 1 Nanoparticle enhanced X-ray radiation killing of MDR bacteria in deep tissue (A), where bacteria are grown underneath a 2 cm thick PMMA block and are irradiated vertically. (B) The scheme showing a combination between bismuth nanoparticles and bacteria.

Using this strategy, MDR *P. aeruginosa*, the leading Gram-negative pathogen in nosocomial infection, has been effectively killed in an environment that simulates human tissues. Bismuth ($Z = 83$) nanoparticles are used in this study because bismuth has the highest X-ray absorption cross-section compared to other heavy metals at any given energy of the incident X-ray photons.[12] Moreover, bismuth derived medicines are known to have low toxicities when administrated for *Helicobacter pylori* eradiation and tumor treatment.[13]

An *in vitro* model is created to validate the microbial killing effect with low dose X-rays by irradiating MDR *P. aeruginosa* grown on a Petri dish that is fixed underneath a 2 cm thick poly(methyl methacrylate) (PMMA) phantom mimicking human tissues. Bismuth nanoparticles are modified with polyclonal antibodies against *P. aeruginosa*, which is followed by incubation with *P. aeruginosa*. After removing unbound nanoparticles by several washes, the bacteria are exposed to X-rays (Fig. 1A). The *in vitro* antimicrobial activity of this method is confirmed using LIVE/DEAD assay, following X-ray irradiation. In addition, the cytotoxicities of antibody functionalized bismuth nanoparticles and X-rays have also been tested on human cell lines.

2 Materials and methods

Materials

The LIVE/DEAD BacLight bacterial viability kit and LIVE/DEAD viability/cytotoxicity kit for mammalian cells are from Invitrogen (Carlsbad, CA). Bismuth nitrate ($Bi(NO_3)_3 \cdot 5H_2O$), sodium borohydride ($NaBH_4$), sodium chloride (NaCl), PMMA, dimethylformamide (DMF), RPMI 1640 culture media, penicillin, streptomycin, fetal bovine serum (FBS), and Dulbecco's phosphate-buffered saline (D-PBS) are from Sigma-Aldrich (St. Louis, MO). Polyvinylpyrrolidone (PVP), 1-ethyl-3-(3-dimethylaminopropyl) carbodiimide (EDC), yeast extract, bacteriological agar, and BD falcon multiwell flat-bottom plate are from VWR (West Chester, PA). Tryptone powder is obtained from MO BIO (Carlsbad, CA). Ultrapure water (18.2 MΩ cm) from a Nanopure System (Barnstead, Kirkland, WA) is used throughout. A Synergy HT multi-mode microplate reader from Biotek (Winooski, VT) is used for absorbance and fluorescence measurements.

P. aeruginosa (ATCC 15442) with a broad spectrum of resistance to various commercial germicides, *Pseudomonas maltophilia* (ATCC 13637), *Pseudomonas fluorescens* (ATCC BAA-477), *Staphylococcus aureus* (ATCC 10832), *Staphylococcus pneumoniae* (ATCC 11733), *E. coli* O157:H7 laboratory strain (ATCC 43895), HeLa (CLL-2) cell line, and MG-63 (CRL-1427) cell line are obtained from American Type Culture Collection (ATCC, Manassas, VA). Polyclonal antibody against *P. aeruginosa* is purchased from Meridian (Memphis, TN). Inverted optical microscopy (ACCU-SCOPE 3032) is used to observe cultured cells and a fluorescence microscope from Olympus (BX51M) is used to take fluorescent images. All chemicals used in this study are of analytical grade and are used without further purification.

Synthesis and characterization of bismuth nanoparticles

Bismuth nanoparticles are synthesized as follows: 0.1 mmol of $Bi(NO_3)_3 \cdot 5H_2O$ and 0.5 mmol PVP are dissolved in 10 ml of DMF. The mixture is degassed with argon under stirring for 15 min. 300 μl of 1 M $NaBH_4$ in water is mixed with 10 ml of DMF and added to the mixture of $Bi(NO_3)_3$ and PVP under vigorous stirring and argon flow for 5 min. The obtained nanoparticles are precipitated by adding acetone, which is followed by centrifugation, washing with acetone and drying in a vacuum.

The morphology of synthesized bismuth nanoparticles is derived using a JEOL 1011 transmission electron microscope (TEM) operated at 100 kV. An X-ray spectrometer (Amptek X-123) with a Si-PIN photodiode is used to analyze XRF emissions from bismuth nanoparticles in the transmission mode. 25 μm thick silver and 250 μm thick aluminum filters are used to reduce the background and improve the signal-to-noise ratio in a low energy (0–15 keV) region of the spectrum. The XRF spectrum for unmodified bismuth nanoparticles is obtained at 40 kV and 100 μA after 2 min irradiation.

Surface modification of nanoparticles and conjugation with polyclonal *P. aeruginosa* antibody

Carboxyl acid group terminated bismuth nanoparticles are obtained by mixing bismuth nanoparticles with 0.5 M PAA solution and stirring for 24 h followed by washing with distilled water for three times. The carboxyl acid modified bismuth nanoparticles are dispersed in phosphate buffer saline (PBS, pH 7.4). For antibody conjugation, the carboxylic-terminated bismuth nanoparticles are allowed to react with the amine groups of *P. aeruginosa* antibodies for 3 h in the presence of EDC, a water-soluble carbodiimide that promotes amide bond formation between carboxylic acid and primary amine. Fig. 1B illustrates the details of the coupling procedure. UV-Vis spectroscopy is carried out using a Varian Cary 500 for absorbance measurement of the antibody. The amount of conjugated antibody is determined by comparing the calibration and the difference between the amount of antibody added to the bacterial suspension and the amount of unbound antibody remaining in the solution. It is assumed that there is no loss

during the conjugation, and the difference between the added antibody and the unbound antibody is the bismuth conjugated antibody. Then the antibody graft density is estimated using the antibody amount and the nanoparticle number (see ESI†). FTIR measurements are carried out using a Thermo-Nicolet Continuum FTIR spectrometer in reflection mode to verify the success of conjugation between bismuth nanoparticle and *P. aeruginosa* antibody. The hydrodynamic diameter of antibody conjugated nanoparticles in PBS is measured by dynamic light scattering (DLS) with a PD2000 DLS detector (Precision Detectors, Amherst, MA).

Cell culture and nanoparticles treatment

HeLa and MG-63 cell lines are used to study cytotoxicity of bismuth nanoparticles. HeLa and MG-63 cells are grown in RPMI 1640 medium supplemented with penicillin (100 units per ml), streptomycin (100 μg ml^{-1}), and 10% fetal bovine serum (FBS) according to the protocol from ATCC. 200 μl cell suspensions are seeded with a final concentration of 1×10^5 cells per ml in each well of a 96-well microplate and cultured in an incubator with 5% CO_2 at 37 °C for 2 days. After the cell monolayer reaches 80% confluence, the medium is changed and cells are incubated with unmodified or antibody functionalized bismuth nanoparticles in fresh medium with the final concentrations of 2, 20, and 200 μg ml^{-1}, respectively. After 48 h, the medium in each well is removed, and the wells are washed with D-PBS prior to viability assay.

Specificity of polyclonal *P. aeruginosa* antibody

The specificity of *P. aeruginosa* antibody is tested by introducing 100 μl of antibody-modified bismuth nanoparticles into 1 ml of bacterial suspensions containing *P. aeruginosa*, *Pseudomonas maltophilia*, *Pseudomonas fluorescens*, *E. coli*, *Staphylococcus aureus*, and *Staphylococcus pneumonia*, respectively. After incubation for 1 h at 37 °C, 100 μl of each bacterial suspension is inoculated and cultured for 24 h in a lysogeny broth (LB) agar plate, followed by XRF measurements before and after washing off the uncombined nanoparticles. The specificity of the bismuth conjugated polyclonal antibody is also verified by incubating the antibody-modified bismuth nanoparticles with cell cultures that contain 80% confluent HeLa or MG-63 cells for 24 h. Then the cell cultures are intensively washed, and XRF spectra of the culture plates are recorded accordingly.

Cytotoxicity assay

Bacterial viability assays are performed using the protocol provided in the bacterial viability kit. For dual staining the bacteria, the bacteria in the broth are diluted to a density of 10^4 CFU ml^{-1} according to the absorbance at 600 nm. 3 μl of the dye mixture (containing an equal volume of green-fluorescent SYTO® 9 stain and red-fluorescent propidium iodide stain) is mixed with 1 ml bacterial suspension and incubated at 37 °C in the dark for 15 min, followed by observation under a fluorescence microscope. For live or dead cell calibration, 0.6 μl of the dye mixture and 200 μl of the bacterial suspension are added into each well of the 96-well microplate. After incubation for 15 min, the fluorescent signals are measured at 530 nm/630 nm (dual fluorescence). The fluorescent backgrounds are subtracted before calculation by measuring a cell-free control. The percentages of live and dead cells are calculated by dividing the fluorescence intensities of live or dead cells by the values obtained for controls.

The bactericidal activity of bismuth nanoparticles (with/without antibody conjugated) is determined by monitoring the growth of *P. aeruginosa* in the presence of bismuth nanoparticles. Briefly, *P. aeruginosa* is grown in LB broth (5 g l^{-1} NaCl, 10 g l^{-1} tryptone powder, and 5 g l^{-1} yeast extract powder, pH 7.4) until a density of $\sim 10^5$ per ml has been reached. Then the bismuth nanoparticles are introduced into the bacterial suspensions at concentrations of 2, 20 and 200 μg ml^{-1}. After 2 h, 100 μl of the bacterial suspension is inoculated and cultured on a LB agar plate for 24 h, followed by counting the colony-forming units (CFUs) of MDR *P. aeruginosa* in the plate.

X-ray irradiation

A Mini-X X-ray tube from Amptek (Bedford, MA) with a silver anode operating at 40 kV and 100 μA is used to produce primary X-rays. The tube is fitted with a brass collimator (with 2 mm diameter pinhole) to focus X-rays onto the target. An X-ray spectrometer (Amptek X-123) with a Si-PIN photodiode is used to analyze XRF emissions in transmission mode. The X-ray spectrometer contains a solid-state detector, a digital pulse processor and a multichannel analyzer, which are interfaced with a computer for data acquisition and analysis. The combination of a 25 μm thick silver filter and a 250 μm thick aluminum filter is used to reduce the background and improve the signal-to-noise ratio in a low energy (0–15 keV) region of the spectrum. The surface dose rate is measured using a handheld radiation dosimeter Mirion RAD-60 from Freshwater Systems (Greenville, SC). In order to derive dose-dependent bactericidal activity of nanoparticles, the X-ray source is fixed at 10 cm from a PMMA phantom ($7 \times 7 \times 2$ cm^3) mimicking the human tissue (ESI, Fig. S1†). MDR *P. aeruginosa* suspension ($\sim 10^5$) in LB medium is taken in a Petri dish which is fixed underneath PMMA, simulating a deeply buried wound with MDR bacterial infection.

To determine the dose enhancement factor (DEF) of the bismuth nanoparticles, different concentrations of antibody modified bismuth nanoparticles solution are mixed with 2 ml of *P. aeruginosa* suspension to get final bismuth nanoparticle concentrations of 2, 20, and 200 μg ml^{-1}, respectively, followed by X-ray irradiation at 40 kV and 100 μA. Control samples without bismuth nanoparticles are also tested under the same conditions. After irradiation, 100 μl of the mixture containing bacteria and nanoparticles is pipetted into a Petri dish and incubated at 5% CO_2 and 37 °C for 24 h until the colony numbers are counted.

To explore the damage of irradiation on mammalian cells, HeLa cells are cultured in a Petri dish and incubated for 2 h with antibody conjugated bismuth nanoparticles at a concentration of 200 μg ml^{-1}. After washing with D-PBS for 3 times, the cultured HeLa cells are irradiated at 40 kV and 100 μA for

different times ranging from 10 min to 120 min. Control samples without bismuth nanoparticles are also tested under the same conditions. Following X-ray exposure, the HeLa cells are subjected to a cell viability test using a LIVE/DEAD viability/cytotoxicity kit according to the provider's protocol (Invitrogen).

The antibacterial activities of *P. aeruginosa* antibody conjugated bismuth nanoparticles and non-conjugated bismuth nanoparticles are studied using *P. aeruginosa* and *E. coli*. Briefly, 200 μl of antibody modified or unmodified bismuth nanoparticles (200 μg ml^{-1}) is added to 200 μl of bacterial suspensions and incubated for 24 h, respectively. After irradiating for 10 min, the bacteria are incubated at 37 °C for 24 h and the colony number is counted.

The penetrating power of 40 kVp X-rays is investigated by stacking several PMMA blocks together and estimating the average number of transmitted X-ray photons. A charged couple device (CCD), interfaced with a computer, is fixed underneath the PMMA block. As X-rays impinge on the CCD, individual X-ray photons are converted into light photons that appear as bright dots on the computer screen. Using customized MATLAB codes, the recorded images are corrected for background and the average number of transmitted X-ray photons is estimated.

Statistical analysis

Six independent duplicates were performed for each test and the data are shown as mean ± standard error. All the figures are plotted using the Origin 8.5 software (OriginLab, Northampton, MA) and statistical analyses were performed using SPSS 16.0 (SPSS Inc, Chicago, Illinois). One-way ANOVA and LSD tests were applied to compare the difference between the numbers of bacterial colony after different treatments. $p < 0.05$ was considered statistically significant.

3 Results and discussion

Bismuth nanoparticles are prepared by a chemical reduction method of bismuth nitrate reported previously.[14] The transmission electron microscopy (TEM) image shows that the nanoparticles have an average diameter of ~30 nm (Fig. 2A). The X-ray fluorescence (XRF) spectrum shows the characteristic $L_\alpha 1$ and $L_\beta 1$ peaks of bismuth at 10.82 and 13.02 keV, respectively (Fig. 2B). The surface of bismuth nanoparticles is oxidized by heating at 120 °C to be modified with silane derivatives.

The polyclonal *P. aeruginosa* antibody is conjugated to the surface of bismuth nanoparticles by carbodiimide chemistry (Fig. 1B). The successful conjugation of the antibody is verified by Fourier transform infrared spectroscopy (FTIR). The presence of C–N peak (1200–1250 cm^{-1}) and NH_2 scissoring peaks (1600–1650 cm^{-1}) in the antibody–bismuth nanoparticle complex confirms conjugation of the *P. aeruginosa* antibody to the nanoparticles (Fig. 2C). The conjugation efficiency of the *P. aeruginosa* antibody with *P. aeruginosa* is estimated by calculating the difference in UV/visible absorptions (280 nm) between the total antibody added and those unbound in the supernatant after centrifugation. The relative amounts of the polyclonal antibody bound to per mg of bismuth nanoparticles are estimated to be ~18.5 μg. Taking the average molecular weight of IgG antibody as 150 kD, the grafting density of the antibody on the nanoparticle surface is estimated to be ~10 (for calculation method see ESI†). The DLS result shows *P. aeruginosa* antibody conjugated bismuth nanoparticles in PBS (pH 7.4) with a size range from 70 to 95 nm and a mean diameter of 82 nm (ESI, Fig. S2†). No obvious aggregates are observed in the antibody modified nanoparticle suspension. These results show that antibody modified nanoparticles are nearly mono-dispersed in PBS with a normal distribution.

The specificity of the antibody–bismuth complex is determined by recording the XRF spectrum after washing away those uncombined nanoparticles. The result shows that ~80% of the original signal is observed in the *P. aeruginosa* culture plate (Fig. 3A), while only ~10% signal in the *E. coli* culture plate can be seen (Fig. 3B) and almost no significant signal is observed in the human adenocarcinoma HeLa cell plate (Fig. 3C), indicating that *P. aeruginosa* antibody modified bismuth nanoparticles can combine with *P. aeruginosa* with high specificity. The weak XRF signal of bismuth in the *E. coli* culture plate is mainly attributed to a small amount of non-specifically attached nanoparticles encapsulated in the bacterial colony. No bismuth XRF peaks are observed in samples containing *Staphylococcus aureus* and

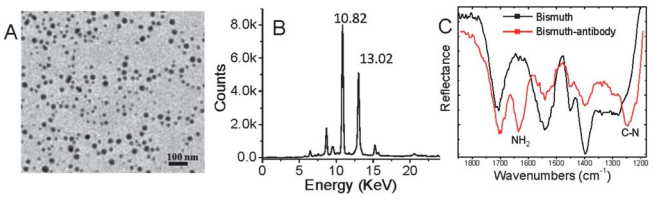

Fig. 2 Synthesized bismuth nanoparticles and their conjugation with antibodies. TEM image (A) and XRF spectrum (B) of bismuth nanoparticles; (C) FTIR spectrum of unmodified and antibody-functionalized bismuth nanoparticles.

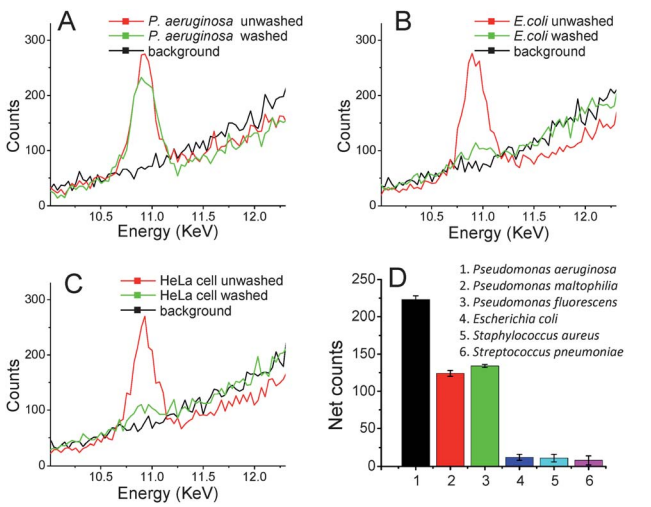

Fig. 3 Specificity of antibody conjugated nanoparticles. (A–C) XRF spectra in the culture of *P. aeruginosa* (A), *E. coli* (B), and HeLa cells (C) after incubating with *P. aeruginosa* antibody-conjugated bismuth nanoparticles for 24 h. Intensive wash was performed prior to XRF measurements. The black, red, and blue lines are background, unwashed samples, and washed samples, respectively. (D) Net XRF counts induced by various bacteria. $N = 6$.

Streptococcus pneumonia (Fig. 3D). Due to cross-linkage, bismuth nanoparticles conjugated with *P. aeruginosa* antibody can also combine with *Pseudomonas maltophilia* and *Pseudomonas fluorescens* by 50% of the strength of *P. aeruginosa*. These results show that the polyclonal *P. aeruginosa* antibody modified bismuth nanoparticles specifically target *P. aeruginosa* instead of other bacteria species or cells, though partial cross-reaction exists between the *P. aeruginosa* antibody and other *Pseudomonas* species.

The toxicity of bismuth nanoparticles has been tested on both HeLa cells and bacteria. Cell viabilities are measured after incubating cells with unmodified or antibody modified bismuth nanoparticles for 24 h. Fig. 4A shows that unmodified bismuth nanoparticles kill 4.6% and 21% of HeLa cells at 2 and 200 μg ml^{-1}, respectively; while *P. aeruginosa* antibody modified bismuth nanoparticles kill 3.2% and 9% of HeLa cells accordingly. The *P. aeruginosa* antibody modified bismuth nanoparticles are less toxic on HeLa cells than unmodified bismuth nanoparticles, probably because unmodified bismuth nanoparticles easily interact with the cells due to their smaller size.[15] The influence of surface modification on the cytotoxicity of the bismuth nanoparticle has been investigated previously.[16]

Apart from their toxic effect on mammalian cells, bismuth nanoparticles also show bactericidal activity. The growth of *P. aeruginosa* in the presence of bismuth nanoparticles has been recorded by counting the number of colony-forming units (CFUs). Fig. 4B shows that antibody-conjugated bismuth nanoparticles kill 14% and 35% of *P. aeruginosa* at a concentration of 2 and 200 μg ml^{-1}, respectively. Meanwhile, the unmodified bismuth nanoparticles only kill 5% and 23% bacteria at a concentration of 2 and 200 μg ml^{-1}, respectively. The antibody functionalized bismuth nanoparticles kill more MDR *P. aeruginosa* cells than HeLa cells because *P. aeruginosa* antibody modified nanoparticles are specifically targeted towards the surface of *P. aeruginosa*, mediating endocytosis of nanoparticles into bacteria cells. It is reported that 2 mM zerovalent bismuth nanoparticles of ~3 nm size have a stronger bactericide effect by killing over 60% *Streptococcus mutans*.[17] This enhanced antimicrobial activity is mainly attributed to their smaller size, making the nanoparticles easier to penetrate the bacterial membrane and induce cell damage.

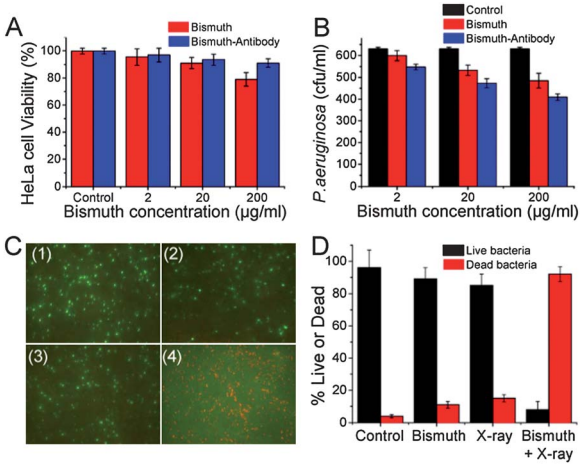

Fig. 4 (A) HeLa cell viability after exposure to different concentrations of bismuth nanoparticles; (B) *P. aeruginosa* cell colony forming unit with different concentrations of bismuth nanoparticles; (C) fluorescent images of the *P. aeruginosa* cell without treatment (1), 40 kVp X-ray treated (2), 200 μg ml^{-1} bismuth nanoparticles treated (3), and both 40 kVp radiation and 200 μg ml^{-1} bismuth treated (4) at 400× magnification; (D) viability of *P. aeruginosa* after different treatments.

All X-ray irradiation are carried out on *P. aeruginosa* suspension at 37 °C for 20 min at 40 kVp and 100 μA (~400 mGy surface dose) with the X-ray source placed at a distance of 10 cm from irradiated samples. The bactericidal activity of bismuth nanoparticle enhanced X-ray radiation is tested by determining bacterial cell viability in LB liquid media immediately after exposure. In addition, X-ray irradiated *P. aeruginosa* LB agar plates are incubated for 24 h and the growth of bacteria is monitored. To evaluate the instant bactericidal activity, LIVE/DEAD® bacterial viability assay is carried out to discriminate dead (stained red) or live (stained green) bacteria. Four types of MDR *P. aeruginosa* samples in LB media are made as follows: (1) untreated MDR *P. aeruginosa* as negative control; (2) radiation treated MDR *P. aeruginosa*; (3) nanoparticle treated MDR *P. aeruginosa*; and (4) radiation and nanoparticle treated MDR *P. aeruginosa*.

Fig. 4C1–C4 show the fluorescent images of the above-mentioned samples (1) to (4), respectively, after 20 min irradiation. Almost all bacterial cells are alive in the negative control (Fig. 4C1); a small amount of dead bacteria are found in 200 μg ml^{-1} bismuth nanoparticle treated bacterial suspension (Fig. 4C2); X-ray irradiated bacterial suspension (Fig. 4C3) also has a few dead bacteria; however, almost all of the bacterial cells are killed after treatment with both radiation and nanoparticle of same dose and same concentration (Fig. 4C4). The percentage of live or dead *P. aeruginosa* from these samples is shown in Fig. 4D, where the combined radiation and nanoparticles kill 92% *P. aeruginosa* cells; X-ray radiation (~400 mGy) alone kills 15% *P. aeruginosa* cells; bismuth nanoparticles (200 μg ml^{-1}) alone kill 10% *P. aeruginosa* cells; only 4% cells are dead in untreated control. These results show that neither X-ray radiation at low dose nor bismuth nanoparticle alone has high bactericidal activity, but the combined use of X-rays and antibody modified bismuth nanoparticles can significantly enhance instant bactericidal activity.

The growth of X-ray irradiated bacteria is monitored by counting the MDR *P. aeruginosa* colonies in the LB agar plate. Results show that the control sample (LB only) has no influence on the bacterial growth (Fig. 5A). The bacteria treated by antibody–bismuth nanoparticles alone (Fig. 5B) or by X-rays alone (Fig. 5C) have fewer colonies than the control. Besides, only a small amount of colony is found after treating by both bismuth nanoparticles and X-rays (Fig. 5D). The colony number (Fig. 5E) shows a decrease of ~19% and ~12% for the X-ray irradiated group and the nanoparticle group, respectively, with respect to the untreated control, while the reduction in the colony number is ~94% in the case of the group treated with both X-rays and nanoparticles. Therefore, the combined use of X-rays and bismuth nanoparticles can significantly reduce the ability of *P. aeruginosa* to reproduce. Above results show that X-ray

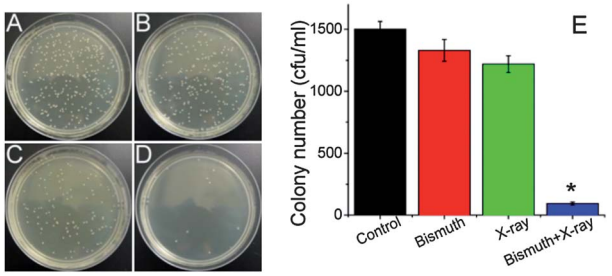

Fig. 5 Images of *P. aeruginosa* cells in the plate without treatment (A), treated with bismuth nanoparticles (B), treated with radiation (C), and treated with both radiation and bismuth nanoparticles (D); counted colony number after different treatment (E). * denotes $p < 0.05$ when compared with non-treated control. $N = 6$.

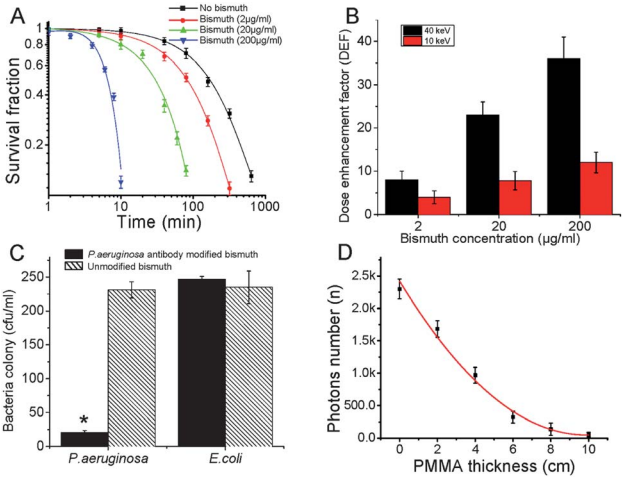

Fig. 6 Nanoparticle enhanced X-ray killing of bacteria. (A) The survival fraction of irradiated *P. aeruginosa* after incubation with different concentrations (2, 20 and 200 μg ml^{-1}) of antibody modified bismuth nanoparticles; (B) the DEF at different nanoparticle concentration; (C) the antimicrobial activities of unmodified and antibody modified bismuth nanoparticles. * denotes $p < 0.05$ when compared with unmodified bismuth nanoparticles. (D) Penetrating ability of 40 kVp X-ray irradiation on a PMMA phantom with a thickness ranging from 0 to 10 cm. $N = 6$.

irradiation decreases bacterial reproduction more than killing the bacteria instantly. This is probably because X-rays damage the double-stranded DNA, which has more influence on decreasing the reproduction capability of bacteria during the double fission process than causing immediate bacterial death.[18] However, the bacteria with severely damaged DNA by acute irradiation are unable to divide and will die eventually.

To mimic *in vivo* bactericidal activity of nanoparticle enhanced radiation, a thin layer of MDR *P. aeruginosa* on a Petri dish (9 cm in diameter) is placed under a 2 cm thick PMMA block that mimics the human tissue. The X-ray source is fixed vertically at a distance of 10 cm from the block. At an output cone angle of 90°, the primary X-ray beam spans over an area of 314 cm^2 on the exposed surface, ensuring that all bacteria are irradiated uniformly. For X-ray irradiation carried out at 40 kV and 100 μA, the measured surface dose rates are 20 and 5.1 mSv min^{-1} at the upper and lower surface of the PMMA block, respectively. Thus, the PMMA block absorbs the primary X-rays at a rate of 14.9 mSv min^{-1}. Assuming PMMA has the same X-ray absorbing properties as skin tissue with a weighing factor of 0.01, the effective dose for PMMA is 0.149 mSv for a 1 min X-ray exposure. This is of the same order of magnitude as the dose in a typical chest X-ray examination (0.1 mSv) and much lower than the dose in an abdominal CT scan (10 mSv).[19]

The bactericidal activity of X-rays is studied with and without the presence of antibody-conjugated bismuth nanoparticles. Fig. 6A shows that the bactericidal activity of X-rays depends on both the irradiation time (dose) and the nanoparticle concentration. In the absence of bismuth nanoparticles, less than 6% bacteria can be killed after 10 min irradiation. However, antibody-conjugated bismuth nanoparticles at concentrations of 2, 20 and 200 μg ml^{-1} kill ~10%, ~15%, and ~90% bacteria, respectively, under the same conditions. These results show that increased nanoparticle concentration can significantly enhance the bactericidal activity of X-rays. The effective dose for skin tissue after 10 min X-ray irradiation is ~1.49 mSv, indicating the relatively less harmful effects of low dose X-rays for short term exposures. This is further verified by studying the effect of X-rays on the viability of HeLa cells containing 200 μg ml^{-1} *P. aeruginosa* antibody conjugated bismuth nanoparticles. Prior to exposure, the cells are washed five times with PBS to remove any unbound nanoparticles. No significant decreases in viabilities of HeLa and MG-63 cells following a 10 min X-ray exposure are observed (data not shown), confirming the less harmful effects of low dose X-rays on mammalian cells. It is clearly shown that 10 min X-ray irradiation has strong bactericidal activity, which is mainly due to the localized dose enhancements provided by the antibody conjugated bismuth nanoparticles that can specifically combine with the bacteria.

The localized dose enhancement is provided by the radiosensitization effect of bismuth nanoparticles as well as the close proximity of the nanoparticles to bacterial cells. Previous Monte Carlo simulation and *in vitro* experiments have shown that the unmodified gold nanoparticles can only enhance the radiation dose by 2–6 times in tumor killing and bacterial deactivation.[20–23] Recent theoretical studies also show that specifically targeted gold nanoparticles can obtain a nucleus DEF of up to 79.[24] Bismuth with a higher X-ray absorption cross-section than gold has a much stronger radiosensitization effect. Upon X-ray irradiation, photoelectrons, secondary X-rays and Auger electrons are generated that deposit most of their energy in the vicinity of nanoparticles. Considering that the radiosensitization effect is stronger if nanoparticles are closer to target cells (within 5 nm) or their DNAs, the antibody modified bismuth nanoparticles can cause more damage to DNA of bacteria, and can enhance localized X-ray dose compared to unmodified bismuth nanoparticles and modified gold nanoparticles.

The DEF is calculated based on the bacterial cell survival curve (Fig. 6A). The DEF is taken as the ratio of the dose that corresponds to 90% survival in the presence of antibody conjugated bismuth nanoparticles at any given concentration and the dose that corresponds to 90% survival without any nanoparticle.[25] Fig. 6B shows that DEFs at 90% survival for 40 keV X-rays are 8, 23, and 35 for 2, 20 and 200 μg ml^{-1}

concentration of bismuth nanoparticles, respectively. For low energy (10 keV) X-rays, DEFs are 4, 8, and 12 for respective concentrations. The DEFs are higher than in a previous report that uses 1 mM of gold nanoparticles and 80 kVp X-rays.[25] This difference could be attributed to two reasons: (i) the total X-ray absorption coefficient of bismuth ($Z = 83$) is 1.2 times higher than that of gold ($Z = 79$) at any given X-ray energy and (ii) antibody-modified bismuth nanoparticles can specifically combine to *P. aeruginosa*, thus greatly enhancing the X-ray killing effect.

To confirm that specifically targeted nanoparticles are the cause of enhanced antibacterial activity, a control experiment is conducted using irradiated *P. aeruginosa* after incubating with 200 μg ml^{-1} of antibody conjugated bismuth nanoparticles and unmodified bismuth nanoparticles, respectively. Fig. 6C shows that antibody modified bismuth nanoparticles kill ~10 times more *P. aeruginosa* than unmodified ones under the same conditions ($p < 0.05$). In contrast, no significant difference in killing *E. coli* is observed for anti-*P. aeruginosa* antibody modified and unmodified bismuth nanoparticles. These results strongly indicate that the increased killing effect from antibody modified bismuth nanoparticles is due to specific binding of nanoparticles to *P. aeruginosa*.

The penetrating power of X-rays is tested using a PMMA phantom with thickness ranging between 2 and 10 cm (ESI, Fig. S2†). PMMA has similar X-ray absorption properties as human tissues and is often used in diagnostic X-ray phantoms.[26] A CCD interfaced to a computer is used to count the number of X-ray photons penetrating through the PMMA phantom. As X-ray photons impinge on the CCD, they are converted to visible light photons, appearing as bright dots on the computer screen. The number of bright dots is proportional to the number of X-ray photons penetrating through PMMA. It is observed that the number of penetrating X-ray photons decreases as the PMMA thickness is increased (Fig. 6D). Results show that 4 cm thick PMMA reduces the number of penetrating X-ray photons by ~50% for 40 kVp X-rays. Therefore, the method is capable of killing bacteria in wounds as deep as 4 cm. The penetration depth of X-rays can be further increased by increasing the tube voltage or placing the X-ray source closer to the targeted wound to reduce attenuation in air.

This study proposes a new strategy for killing of MDR bacteria using bismuth nanoparticle-enhanced X-ray radiation. Although the proposed method shows promising capabilities for treatment of deeply buried wound infections, further improvements are warranted before it can be put into clinical use. The harmful effects of low dose X-rays should be fully addressed by determining the genotoxicity of long term radiation exposure using animal models. The inherent toxicity associated with the bismuth nanoparticles can be reduced by using appropriate surface coatings such as polyethylene glycol. After irradiation, the wound should be thoroughly washed with alcohol to remove dead bacteria or any unbound nanoparticles. For complete removal of the nanoparticles from the body, the particle size can be reduced to ~5 nm or less to facilitate the clearance from kidneys for future *in vivo* applications.

4 Conclusions

A new approach is developed to kill MDR bacteria by nanoparticle enhanced X-ray irradiation. The high penetrating power of X-rays allows killing of bacteria in deep tissues to prevent wound infection. The use of high Z nanoparticles provides significant localized dose enhancements of 35 times in microbial killing, whereas, mammalian cells are not significantly affected under these conditions. Although MDR *P. aeruginosa* is used in this study, the method can be developed to kill other types of microorganisms in human wounds by conjugating respective antibodies onto nanoparticles.

Acknowledgements

This project has been supported by a research grant (0828466) and a CAREER award from National Science Foundation, a Concept Award (W81XWH-10-1-0961) from Lung Cancer Research Program of Department of Defense, a grant from the National Natural Science Foundation of China (30900348), and a fund for the Transformation of Scientific and Technological Achievements of the Third Military Medical University (2010XZH08).

Notes and references

1 D. Li, J. Diao, J. Zhang and J. Liu, *J. Nanosci. Nanotechnol.*, 2011, **11**, 4733–4738.
2 W. C. Huang, P. J. Tsai and Y. C. Chen, *Nanomedicine*, 2007, **2**, 777–787.
3 Y. Y. Zhao, Y. Tian, Y. Cui, W. W. Liu, W. S. Ma and X. Y. Jiang, *J. Am. Chem. Soc.*, 2010, **132**, 12349–12356.
4 W. C. Huang, P. J. Tsai and Y. C. Chen, *Small*, 2009, **5**, 51–56.
5 N. Ren, R. Li, L. M. Chen, G. C. Wang, D. Liu, Y. J. Wang, L. Zheng, W. Tang, X. Q. Yu, H. D. Jiang, H. Liu and N. Q. Wu, *J. Mater. Chem.*, 2012, **22**, 19151–19160.
6 S. Lehnert and H. Moroson, *Radiat. Res.*, 1971, **45**, 299–310.
7 M. E. Werner, J. A. Copp, S. Karve, N. D. Cummings, R. Sukumar, C. Li, M. E. Napier, R. C. Chen, A. D. Cox and A. Z. Wang, *ACS Nano*, 2011, **5**, 8990–8998.
8 L. Wang, W. Yang, P. Read, J. Larner and K. Sheng, *Nanotechnology*, 2010, **21**, 475103.
9 T. Kong, J. Zeng, X. Wang, X. Yang, J. Yang, S. McQuarrie, A. McEwan, W. Roa, J. Chen and J. Z. Xing, *Small*, 2008, **4**, 1537–1543.
10 A. Simon-Deckers, E. Brun, B. Gouget, M. Carriere and C. Sicard-Roselli, *Gold Bull.*, 2008, **41**, 187–194.
11 R. S. Norman, J. W. Stone, A. Gole, C. J. Murphy and T. L. Sabo-Attwood, *Nano Lett.*, 2008, **8**, 302–306.
12 O. Rabin, J. Manuel Perez, J. Grimm, G. Wojtkiewicz and R. Weissleder, *Nat. Mater.*, 2006, **5**, 118–122.
13 P. Malfertheiner, F. Bazzoli, J. C. Delchier, K. Celinski, M. Giguere, M. Riviere and F. Megraud, *Lancet*, 2011, **377**, 905–913.
14 M. Hossain, Y. Luo, Z. Sun, C. Wang, M. Zhang, H. Fu, Y. Qiao and M. Su, *Biosens. Bioelectron.*, 2012, **38**, 348–354.

15 A. Hoshino, S. Hanada and K. Yamamoto, *Arch. Toxicol.*, 2011, **85**, 707–720.
16 Y. Luo, C. Wang, M. Hossain, Y. Qiao, L. Ma, J. An and M. Su, *Anal. Chem.*, 2012, **84**, 6731–6738.
17 R. Hernandez-Delgadillo, D. Velasco-Arias, D. Diaz, K. Arevalo-Nino, M. Garza-Enriquez, M. A. De la Garza-Ramos and C. Cabral-Romero, *Int. J. Nanomed.*, 2012, **7**, 2109–2113.
18 M. Tomita, F. Morohoshi, Y. Matsumoto, K. Otsuka and K. Sakai, *J. Radiat. Res.*, 2008, **49**, 557–564.
19 B. F. Wall and D. Hart, *Br. J. Radiol.*, 1997, **70**, 437–439.
20 J. M. Kinsella, R. E. Jimenez, P. P. Karmali, A. M. Rush, V. R. Kotamraju, N. C. Gianneschi, E. Ruoslahti, D. Stupack and M. J. Sailor, *Angew. Chem., Int. Ed.*, 2011, **50**, 12308–12311.
21 C. J. Liu, C. H. Wang, C. C. Chien, T. Y. Yang, S. T. Chen, W. H. Leng, C. F. Lee, K. H. Lee, Y. Hwu, Y. C. Lee, C. L. Cheng, C. S. Yang, Y. J. Chen, J. H. Je and G. Margaritondo, *Nanotechnology*, 2008, **19**, 295104.
22 E. Brun, L. Sanche and C. Sicard-Roselli, *Colloids Surf., B*, 2009, **72**, 128–134.
23 B. L. Jones, S. Krishnan and S. H. Cho, *Med. Phys.*, 2010, **37**, 3809–3816.
24 W. Ngwa, G. M. Makrigiorgos and R. I. Berbeco, *Med. Phys.*, 2012, **39**, 392–398.
25 W. N. Rahman, N. Bishara, T. Ackerly, C. F. He, P. Jackson, C. Wong, R. Davidson and M. Geso, *Nanomedicine*, 2009, **5**, 136–142.
26 R. Sharma, S. D. Sharma, Y. S. Mayya and G. Chourasiya, *Radiat. Prot. Dosim.*, 2012, **151**, 379–385.

